PERGAMON

International Journal of Multiphase Flow 28 (2002) 927–941

International Journal of Multiphase Flow

www.elsevier.com/locate/ijmulflow

Two-phase pressure drop, boiling heat transfer, and critical heat flux to water in a small-diameter horizontal tube

W. Yu [a,*], D.M. France [b,1], M.W. Wambsganss [a], J.R. Hull [a]

[a] *Energy Technology Division, Argonne National Laboratory, 9700 S. Cass Avenue, Building 335, Argonne, IL 60439, USA*

[b] *Department of Mechanical Engineering, University of Illinois at Chicago, M/C 251, 842 W. Taylor Street, Chicago, IL 60607-7022, USA*

Received 6 September 2001; received in revised form 30 January 2002

Abstract

Two-phase pressure drop, boiling heat transfer, and critical heat flux to water were studied in a small horizontal tube of 2.98-mm inside diameter and 0.91-m heated length. Experiments were performed at a system pressure of 200 kPa, mass fluxes of 50–200 kg/m^{2}s, and inlet temperatures from ambient to 80 °C. Experimental results and comparisons with state-of-the-art predictive correlations are presented. Modifications were made to the Chisholm two-phase multiplier correlation and to the Argonne National Laboratory small-channel boiling heat transfer correlation to better predict the experimental data of the present study.

Keywords: Pressure drop; Boiling heat transfer; Critical heat flux; Small channel; Horizontal flow

1. Introduction

Compact heat exchangers are used extensively in various fields. Some of these exchangers work under two-phase boiling conditions. From the standpoint of design and application, the avoidance of critical heat flux (CHF) is extremely important for these kinds of exchangers. However, studies on this subject are very few. It is the purpose of our ongoing investigations to experimentally investigate the boiling characteristics of heat transfer of water, ethylene glycol, and their

* Corresponding author. Tel.: +1-630-252-6153; fax: +1-630-252-5568.

E-mail addresses: wyu@anl.gov (W. Yu), dfrance@uic.edu (D.M. France), wambsganss@anl.gov (M.W. Wambsganss), jhull@anl.gov (J.R. Hull).

[1] Tel.: +1-312-996-0520; fax: +1-312-996-8664.

0301-9322/02/$ - see front matter
PII: S0301-9322(02)00019-8

mixtures under conditions of horizontal flow, small channel, and low mass flux. This paper reports results on two-phase pressure drop, boiling heat transfer, and CHF when water is used as the experimental fluid.

Two-phase pressure drop has been a research subject for several decades. The most frequently used analysis methods are based on the concept of two-phase multipliers proposed by Lockhart and Martinelli (1949) and the fitting correlation of the multipliers from Chisholm (1967, 1973). Although later investigators have noted that the two-phase multipliers also vary systematically with mass flux, the basic approach of Lockhart and Martinelli remains widely used. The number of times their parameter appears in various contexts in the study of two-phase flow is a strong testament to its worth. This method is used in analyzing the two-phase pressure drop data of the present study.

Many studies on boiling heat transfer are reported in the open literature, and prediction correlations for various application fields are available (ASHRAE, 1993). Among various prediction correlations, two, those of the Chen (1966) and the Argonne National Laboratory (ANL) (Tran et al., 1996), were selected for comparison with the experimental data. As one of the most cited, the Chen correlation can be used for both vertical and horizontal flows. The ANL correlation is based on experimental results obtained with refrigerants in small channels, a circumstance that is analogous to the present study.

Studies on CHF are mostly based on conditions of vertical flow, large channel, high pressure, and high mass flux (Tong, 1972). Predictive methods for CHF in horizontal flow are scarce and inaccurate, and no theoretically based predictive procedure is now available for horizontal flow at low mass fluxes (Weisman, 1992; Wong et al., 1990). In this paper, CHF data are compared with the predicted values of the Groeneveld–Cheng–Doan method, which is based on an 8-mm-diameter CHF lookup table and uses correlation factors to various diameters and horizontal flows (Groeneveld et al., 1986).

2. Experimental apparatus and test procedure

The test apparatus used in this investigation was designed and fabricated to study two-phase pressure drop, boiling heat transfer, and CHF of flowing water, ethylene glycol, and aqueous mixtures of ethylene glycol at high temperatures (up to 250 °C) and low pressure (<345 kPa). Most of the piping system was fabricated from 6.35-mm-diameter brass tubing (0.79-mm wall thickness) and Swagelok fittings.

2.1. Two-phase loop

As shown in Fig. 1, fluid is pumped through the loop and pressurized by an expansion tank connected to a high-pressure nitrogen bottle. Pressure at the experimental test section is maintained within specifications by adjusting the pressure in the expansion tank.

A rotameter and a turbine-type flowmeter are arranged in a parallel-flow configuration to measure two ranges of volumetric flow rate. A temperature sensor just upstream from the flowmeters provides a means to determine fluid density and, subsequently, the mass flow rate of the fluid. Fine adjustment of the fluid flow rate is accomplished with an AC adjustable-frequency drive.

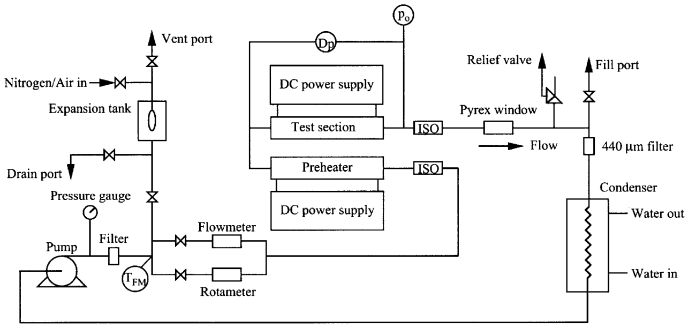

Fig. 1. Schematic diagram of critical-heat-flux test apparatus.

Exiting the flowmeters, the fluid flows through a system preheater in which the fluid temperature is raised to a desired subcooled level for a given test. The preheater consists of a Type 304 stainless steel tube with 4.57-mm inside diameter, 6.10-mm outside diameter, and 500-mm length. Direct current at low voltage from a regulated power supply is passed through the preheater tube wall to generate resistance heat. The power supply output regulation range is 0.1% of the voltage or current and has a power capability of up to 10 kW.

After passing through the preheater, the fluid enters the experimental test section, shown schematically in Fig. 2. The test section is resistance heated with DC by a separate regulated power supply (maximum output: 18 kW) from the preheater. Voltage drop across the test section is measured directly, and the current is determined from a measurement of the voltage drop across a shunt resistor. Power (heat) input to the test section is calculated as the product of the voltage drop and the current. Immediately beyond the experimental test section, a Pyrex window provides a view of the flow pattern. Electrical isolation of the preheater/test-section arrangement, for the purpose of eliminating ground loops, is provided by short sections of high-pressure hose, designated ISO (for isolation) in Fig. 1.

The test section is well insulated thermally from the atmosphere to minimize heat loss to the environment. However, test-section heat loss calibration tests were performed, and the slight heat loss was subsequently incorporated into the data reduction.

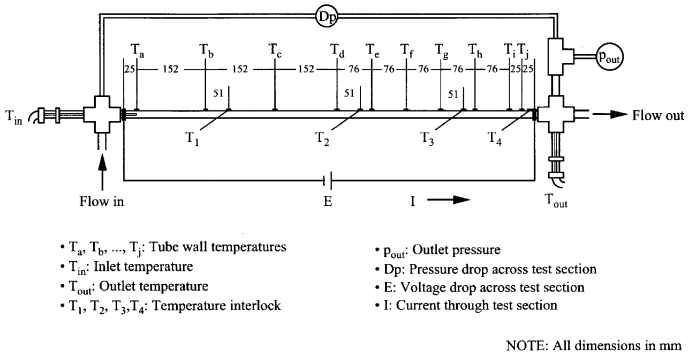

Fig. 2. Schematic diagram of test section.

Fluid leaves the test section as a two-phase flow and is condensed in the counter-current condenser that uses laboratory water as a heat rejection fluid. The condensate leaves the condenser and returns to the pump, closing the system loop.

2.2. Test section

The test section, shown schematically in Fig. 2, was fabricated from 2.98-mm-inside-diameter Type 316 stainless steel tubing with a 4.76-mm outside diameter. The heated length is 0.91 m.

The in-stream bulk fluid temperature is measured at the inlet (T_{in}) and outlet (T_{out}) of the test section. A Type K thermocouple probe, which does not significantly affect the flow because it has a very small outside diameter of 1.57 mm, was selected to measure the inlet bulk fluid temperature. (The probe occupied 28% of the flow area.)

Fig. 2 also illustrates the method used to measure wall temperatures ($T_a, T_b, \ldots, T_j$), which were measured at 10 axial locations over the heated length of the test section with Type K thermocouples. To electrically isolate these thermocouples from the tube, a thin coat of high-temperature ceramic epoxy was applied around the circumference of the tube at the measurement points. After oven curing, the thermocouple junctions were coated with the same high-temperature ceramic epoxy and bonded to the thin coating on the tube. This technique allowed the thermocouple junctions to be electrically insulated from the test-section tube through which current was passing. All thermocouples (wall and stream) were calibrated before installation.

Outlet fluid pressure (p_{out}) and overall pressure drop (Δp) across the test section were measured in all tests. These measurements were incorporated in the data reduction to calculate stream temperature distribution along the boiling segment of the test section.

As a safety precaution, the test section was provided with four high-temperature limit interlocks. Wall temperatures (T_1, T_2, T_3, T_4) are measured at 0.22, 0.53, and 0.76 m from the inlet, and near the outlet of the test section; they are then input to a high-temperature limit switch that terminates power to the test section when a preset upper-temperature limit is reached. The interlocks protect the test section from overheating due to CHF and/or transition boiling leading to a prolonged dry wall condition.

2.3. Data acquisition

A data acquisition system consisting of a PC and multiplexor was assembled to record outputs from all sensors. A data acquisition code, which includes all calibration equations and conversions to desired engineering units, was written to provide on-screen display of analog signals from all sensors and graphs of representative in-stream and wall-temperature measurements. These graphed signals were visually monitored to determine when steady state was achieved. Once that determination was made, all sensor-output voltages were read 15 times by the data acquisition system and then averaged in three sets of five data scans each. As a check on steady state, the three data sets were compared for consistency before all of the scans were averaged together for future processing. The final result was a set of measurements, each an average of 15 readings, plus a confirmation of steady-state system operation during the collection of data.

Included in the final set of averaged measurements was pertinent information such as input power, mass flux, outlet pressure, test-section pressure drop, and outlet quality. These parameters were also displayed on the data acquisition system screen that allowed the facility operator to set up a particular test.

2.4. Test procedure

A series of experiments investigated the characteristics of two-phase pressure drop, boiling heat transfer, and CHF under conditions of horizontal flow, small channel, and low mass flux. Tests were performed at a system pressure of 200 kPa, mass flux range of 50–150 kg/m^{2}s, and inlet temperature range of ambient to 80 °C.

Each CHF measurement was the result of a set of tests. In these tests, the preheater power supply was set to a certain level to keep the inlet temperature of the test section at a desired point. The test-section power supply was increased progressively (in small increments, with data recorded at each step) until the CHF was reached.

The local boiling heat transfer coefficient $h(z)$ was calculated from the equation

$$h(z) = \frac{q''}{T_w(z) - T_{sat}(z)}, \tag{1}$$

where the local wall temperature $T_w(z)$ was measured indirectly, the local saturation temperature $T_{sat}(z)$ was determined from the two-phase pressure drop and exit saturation temperature measurement, and the heat flux at the inside surface of the test channel, q'', was calculated from input power and heat loss. The wall temperature at the inside surface, $T_w(z)$, was determined from a one-dimensional (radial) heat conduction model with measured heat generation in the wall and measured outside surface temperature. Also, the two-phase pressure drop in the test section was small in all experiments (less than 40 kPa). Thus, the pressure was assumed linear with very little error.

Uncertainties for experimental results were determined by using the method of sequential perturbation, as outlined by Moffat (1988) for single-sample data. Uncertainties in each of the independent variables used to calculate the two-phase pressure drop and heat transfer coefficient were estimated on the basis of calibration and examination of system/sensor interaction errors. The uncertainties are $<5\%$ for the experimental results.

3. Validation of test system

To characterize the CHF heat transfer test apparatus, we conducted a series of heat loss, single-phase heat transfer, and single-phase pressure drop tests.

3.1. Heat loss

Although the test section was well insulated to minimize heat loss to the environment, the heat loss was not negligible during the tests because of the low flow rates and high driving temperatures. Heat loss was determined through a special series of experiments in which there was no fluid in the test section. Power was applied to the test section to bring it to a selected temperature. The input

power required to maintain the wall temperature at the selected value is the heat loss q_{env}, which corresponds to the driving temperature difference between the test section and ambient, ΔT_{amb}.

The heat loss based on these tests produced a linear relationship between q_{env} and and ΔT_{amb} as

$$q_{env} = \alpha \Delta T_{amb}, \tag{2}$$

where α is a constant dependent on the heat transfer coefficient and the heat transfer surface area between the test section and ambient for this particular test section. In all of the tests, the heat loss around the test section was <5%. This loss was included in the data reduction of heat transfer tests.

3.2. Single-phase heat transfer and pressure drop

Single-phase heat transfer and pressure drop tests were performed at system pressures of 138 and 200 kPa, sufficient to keep the fluid in the liquid phase during heating. The results of the single-phase heat transfer coefficients for turbulence Reynolds numbers in the range of 2800–7700 were in good agreement (all data were ±20%) with both the Dittus–Boelter correlation (Dittus and Boelter, 1930) and the Petukhov–Popov correlation (Petukhov, 1970); see Fig. 3 in which the local Nusselt numbers are plotted. The Dittus–Boelter correlation and the Petukhov–Popov correlation are given, respectively, as

$$Nu = 0.023 Re^{0.8} Pr^{0.4} \tag{3}$$

and

$$Nu = \frac{(f/8) Re\, Pr}{1 + 3.4f + (11.7 + 1.8/Pr^{1/3})(f/8)^{1/2}(Pr^{2/3} - 1)}, \tag{4}$$

where Re is the Reynolds number, Pr is the Prandtl number, and f is the predicted Fanning friction factor, which can be defined as

$$f = (1.82 \log Re - 1.64)^{-2}. \tag{5}$$

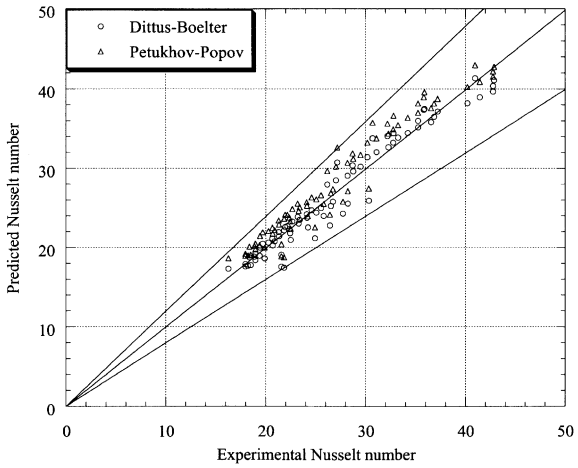

Fig. 3. Single-phase heat transfer data compared with Dittus–Boelter and Petukhov–Popov equations.

The Fanning friction factors calculated from the experimental pressure drop data were in good agreement with standard correlations, e.g. Blasius. These single-phase pressure drop and single-phase heat transfer test results verified the accuracy of the instrumentation, measurements, data acquisition, and data reduction procedures.

4. Experimental results and analysis

4.1. Boiling curve

Boiling heat transfer test results at the test-section outlet are shown in Fig. 4 at a fixed mass flux of 103 kg/m^{2}s and four liquid inlet temperatures to the test section. At any given inlet temperature, the symbols correspond to the steps in the test procedure (described previously) where heat flux was increased incrementally. The portion of the results below a wall superheat of ≈8 °C corresponds to typical high heat flux (or nucleate type) boiling. At higher wall superheats, the wall temperature showed oscillations indicative of transition boiling, and the highest superheat point for each symbol plotted in Fig. 4 is the CHF limit for that inlet temperature. Increasing the heat flux beyond the CHF caused an excursive instability. The wall temperature rose rapidly, and the test was automatically terminated. (The data below 8 °C in Fig. 4 were used in conjunction with flow boiling heat transfer correlations discussed subsequently.)

The results of Fig. 4 show that wall superheat dependence on heat flux is somewhat insensitive to the inlet fluid temperature in the nucleate type boiling regime below 8 °C wall superheat. The CHF point, however, does show such a dependence. This result has implications for the heat transfer coefficient and the correlation of results discussed subsequently.

Shown in Fig. 5 is a superposition of plots similar to that of Fig. 4 at five values of mass flux. The inlet fluid temperature is from ambient to 80 °C. (Change in inlet temperature caused a change in the boiling length as calculated from a heat balance.) It is observed at low wall superheats (below 10 °C) that the data are nearly independent of mass flux. The CHF is clearly a

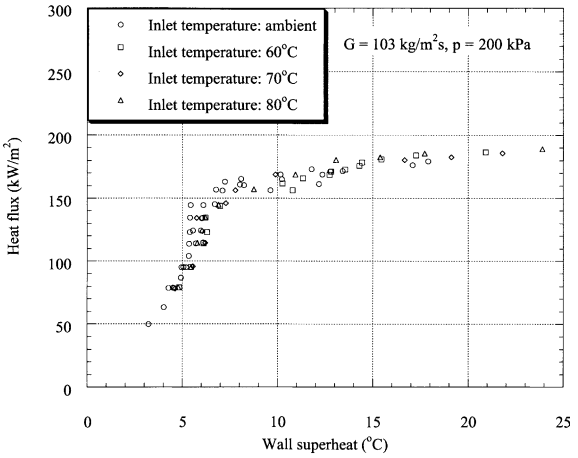

Fig. 4. Heat flux as a function of wall superheat in CHF experiments (inlet temperature effect).

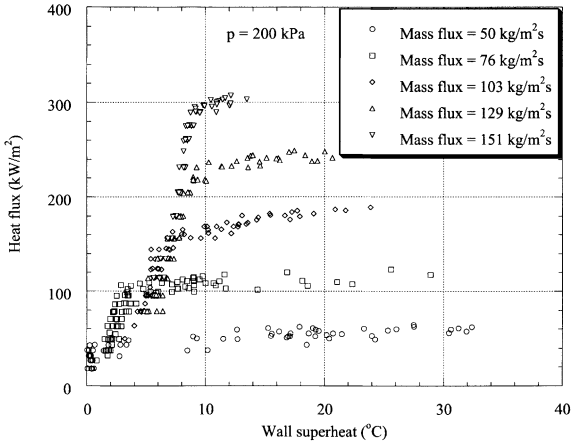

Fig. 5. Heat flux as a function of wall superheat in CHF experiments (mass flux effect).

function of mass flux, but the boiling data are not. This result, coupled with the inlet temperature result, implies that the heat transfer coefficient up to transition boiling is a function of heat flux only. Mass flux and inlet temperature effects are minimal. This result, which is the same as recent findings for boiling refrigerants in small channels with length about 1 m (Tran et al., 1996), was attributed to the large-slug-flow regime found in small-channel two-phase flow (Wambsganss et al., 1992), which gives rise to domination of the nucleation heat transfer mechanism and the minimization of the convective mechanism over a large mass flux and quality range. This result was important to the correlation of data presented subsequently.

In contrast to the two-phase boiling heat transfer results that show heat flux as the only dominant independent variable, the CHF results of Fig. 5 show a dependence on heat flux, mass flux, and inlet subcooling. These findings were considered in the subsequent correlation of the CHF data.

4.2. Two-phase pressure drop

Two-phase pressure drop was measured for each test in the CHF experimental series. The frictional pressure gradient data were analyzed by using the concept of two-phase multipliers. Two multipliers used in this study are

$$\phi_{\mathrm{FL}}^2 = Dp_{\mathrm{exp}}/Dp_{\mathrm{FL}} \tag{6}$$

and

$$\phi_{\mathrm{FLO}}^2 = Dp_{\mathrm{exp}}/Dp_{\mathrm{FLO}}, \tag{7}$$

where Dp_{exp} is the measured two-phase pressure gradient, and Dp_{FL} and Dp_{FLO} are the frictional gradients that correspond, respectively, to the cases of the liquid flowing alone in the channel and the total mixture flowing as a liquid.

The two-phase friction multiplier ϕ_{FLO}^2 is plotted in Fig. 6 against exit mass quality x. The effects of both mass flux and quality are to increase ϕ_{FLO}^2, as clearly displayed in Fig. 6.

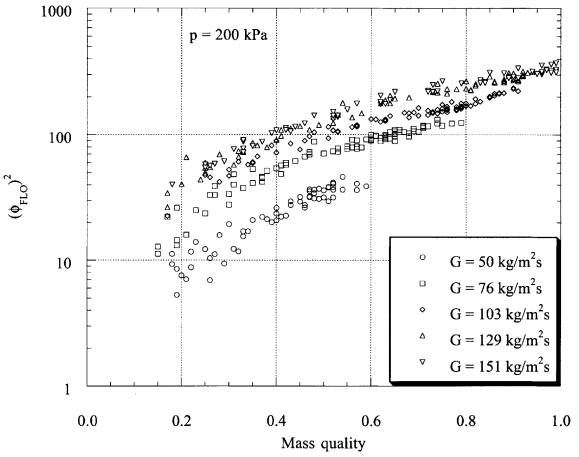

Fig. 6. Two-phase frictional pressure gradient as a function of mass quality.

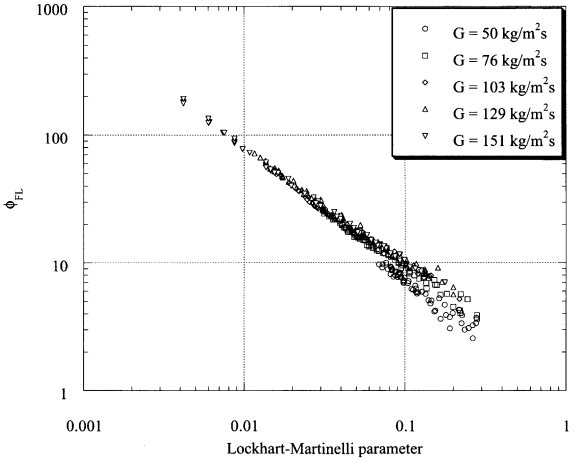

Fig. 7. Two-phase frictional pressure gradient as a function of Lockhart–Martinelli parameter.

In correlating the two-phase friction data, the Lockhart and Martinelli approach (Lockhart and Martinelli, 1949) was used. Accordingly, the two-phase friction multiplier ϕ_{FL} is plotted in Fig. 7 against the Lockhart–Martinelli parameter X, where

$$X = (Dp_{FL}/Dp_{FV}) \tag{8}$$

and Dp_{FV} is the frictional pressure gradient that corresponds to the case of the vapor flowing alone in the channel. Over the range of the mass flux tested in this study, the flow regimes associated with the liquid flowing alone and the vapor flowing alone are laminar and turbulent, respectively. Therefore, in this study the Lockhart–Martinelli parameter becomes

$$X = 18.65\left(\frac{\rho_G}{\rho_L}\right)^{0.5}\left(\frac{1-x}{x}\right)\frac{Re_G^{0.1}}{Re_L^{0.5}}, \tag{9}$$

where ρ is the phasic density and x is the test-section exit quality. The results shown in Fig. 7 indicate that the Lockhart–Martinelli parameter is a single correlating parameter for two-phase friction. This is the same quantitative condition that occurs in large tubes, although the qualitative results for small tubes were expected to differ because of associated two-phase flow regimes.

To correlate the two-phase multiplier of Fig. 7, the Chisholm correlation (Chisholm, 1967, 1973)

$$\phi_{\mathrm{FL}}^2 = 1 + \frac{C}{X} + \frac{1}{X^2} \tag{10}$$

was employed. In Eq. (10), C is a constant that depends on the laminar/turbulent flow regimes of all liquid or vapor flow. In the present study, with laminar liquid phase and turbulent vapor phase, the constant C is 12 in the Chisholm correlation. The experimental two-phase frictional pressure gradient data are compared with the predictions of the Chisholm correlation in Eq. (10), where it is seen that the correlation consistently over predicts the data (open symbols) with an rms error of 33%. The occurrence of slug flow over a large quality range in small channels reduces the pressure gradients from the annular flow condition found in large tubes upon which the Chisholm correlation is substantially based. Looking at the three terms of the Chisholm correlation, we found that the $1/X^2$ term was dominant with the present data and that the data were then better correlated with a power function

$$\phi_{\mathrm{FL}}^2 = X^{-1.9}. \tag{11}$$

This result is shown in Fig. 8 as solid symbols, and the comparison is considered good with an rms error of 7%. In previous small-channel experiments with refrigerant flow (Wambsganss et al., 1992), the Chisholm correlation was found to predict the data better if all three terms were retained and the C coefficient was correlated as a function of the Lockhart–Martinelli parameter and mass flux. In the present investigation with water, all of the data were in the laminar liquid/turbulent vapor regime, and the simple correlation given by Eq. (10) predicted the data well.

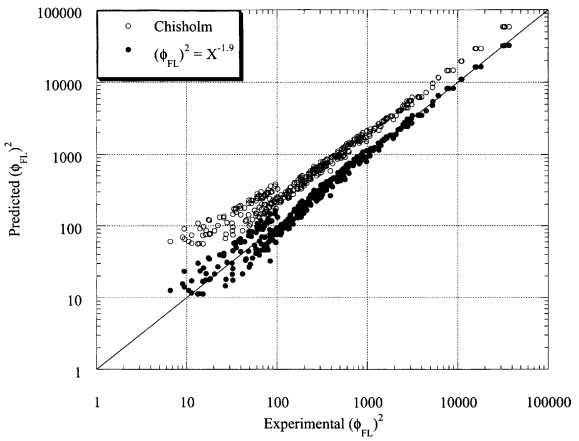

Fig. 8. Two-phase frictional pressure gradient data compared with predicted equations.

4.3. Boiling heat transfer coefficient

The Chen correlation for the boiling heat transfer coefficient has been used for many years for water flowing in tubes larger than the 2.98-mm-diameter tube of the present study. Chen was the first to introduce the superposition approach of nucleation and forced convection mechanisms. The convective transfer is expressed as a function of the two-phase Reynolds number after Lockhart–Martinelli, and the nucleation transfer is obtained from the nucleate boiling correlation of Forster and Zuber (1955). The Chen correlation can be expressed as

$$h = 0.00122\frac{K_{\mathrm{l}}^{0.79}C_{p\mathrm{l}}^{0.45}\rho_{\mathrm{l}}^{0.49}}{\sigma^{0.5}\mu_{\mathrm{L}}^{0.29}i_{\mathrm{fG}}^{0.24}\rho_{\mathrm{v}}^{0.24}}\Delta T_{\mathrm{sat}}^{0.24}\Delta p_{\mathrm{sat}}^{0.75}S + 0.023\left[\frac{G(1-x_z)D}{\mu_{\mathrm{L}}}\right]^{0.8}\left(\frac{\mu C_p}{K}\right)_{\mathrm{l}}^{0.4}\frac{K_{\mathrm{l}}}{D}F, \tag{12}$$

where G is the mass flux, D is the diameter, h_{GL} is the latent heat of vaporization, C_p is the specific heat, x_z is the local quality, μ is the viscosity, K is the thermal conductivity, σ is the surface tension, ΔT_{sat} is the wall superheat, Δp_{sat} is the difference between the saturation pressures calculated from the wall temperature and the fluid temperature, parameter S is calculated as

$$S = \frac{1}{1 + 2.53\times 10^{-6}F^{1.25}G(1-x)D/\mu_{\mathrm{L}}}, \tag{13}$$

and parameter F is calculated as

$$F = \begin{cases} 1.0 & 1/X_{\mathrm{tt}} \leqslant 0.1, \\ 2.35(1/X_{\mathrm{tt}} + 0.213)^{0.736} & 1/X_{\mathrm{tt}} > 0.1, \end{cases} \tag{14}$$

where X_{tt} is the turbulent–turbulent Lockhart–Martinelli parameter

$$X_{\mathrm{tt}} = \left(\frac{1-x}{x}\right)^{0.9}\left(\frac{\rho_{\mathrm{G}}}{\rho_{\mathrm{L}}}\right)^{0.5}\left(\frac{\mu_{\mathrm{L}}}{\mu_{\mathrm{G}}}\right)^{0.1}. \tag{15}$$

Fig. 9 shows the experimental results of local boiling heat transfer coefficients and the predicted values of the Chen correlation. The Chen correlation is based on water results in relatively large channels and produced predictions of the small channel water data of this study that are well centered in the data, with scatter somewhat above ±30% and an rms error of 6%. In an attempt to evaluate the channel size effect, the data were compared with a correlation developed for refrigerant flow boiling in small channels.

Based on the experimental results of boiling heat transfer with two refrigerants in small channels, Tran et al. (1996) found that the dominant mechanism of boiling heat transfer in small channels is nucleation. This situation was found to be a consequence of the large-slug-flow regime in small channels. They then correlated boiling heat transfer coefficients as a function of boiling number B_{o}, liquid Weber number We_{L}, and density ratio $\rho_{\mathrm{L}}/\rho_{\mathrm{G}}$. A similar trend was observed in the present study. Following the approach of Tran et al. (1996), the local boiling heat transfer coefficient was correlated as follows:

$$h = 6400000(B_{\mathrm{o}}^2We_{\mathrm{l}})^{0.27}(\rho/\rho)^{-0.2}, \tag{16}$$

where the Boiling and Weber numbers are given, respectively, as

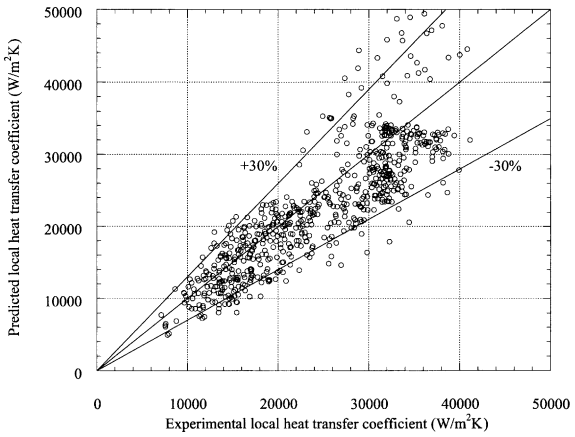

Fig. 9. Boiling heat transfer data compared with Chen equation.

$$B_o = \frac{q''}{Gh_{LG}} \tag{17}$$

and

$$We_L = \frac{G^2 D}{\rho_L \sigma}. \tag{18}$$

Fig. 10 shows the experimental data and the predicted values obtained with Eq. (16). The predictions of Eq. (16) are in good agreement with the present experimental data, and the rms error is 2% that is less than that of the Chen correlation predictions.

The success of Eq. (16) in predicting the heat transfer coefficient is directly related to the trends presented previously in Figs. 4 and 5. Eq. (16) is heat flux and not mass flux dependent as are the data, and the data of Figs. 9 and 10 used in comparison with correlations appropriately exclude the transition boiling regime. It should be noted that the Chen correlation predicts the data best when the nucleation term dominates over the convective term in concert with the data trend. The

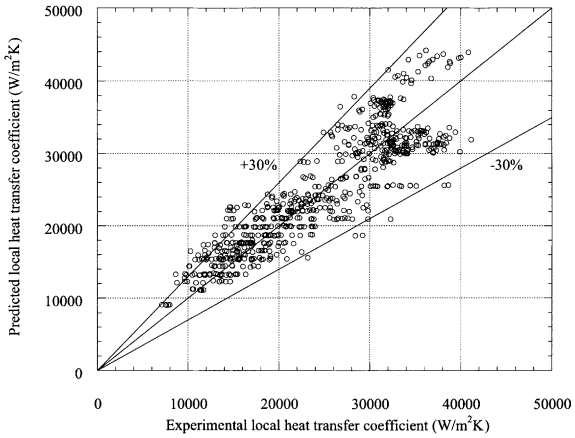

Fig. 10. Boiling heat transfer data compared with modified ANL equation.

small-channel heat transfer data in both water and refrigerants show heat flux and not mass flux dependence up to high qualities (above 0.5) when compared with large-tube conditions.

4.4. Critical heat flux

Considerable research work has been performed on predictive methods for CHF in vertical flow. In comparison, predictive methods for CHF in horizontal flow are scarce, especially at low mass flux as in this study. One predictive method, proposed by Groeneveld et al. (1986) for CHF in horizontal flow that includes the parameter range of the current data, is based on correction of the results of CHF in vertical flow as

$$q''_{\text{hor}} = K_{\text{hor}} q''_{\text{table}}, \tag{19}$$

where q''_{table} is the CHF value obtained from a lookup table, K_{hor} is the correction factor that can be expressed as a linear function of the mass flux

$$K_{\text{hor}} = \begin{cases} 0.0 & G \leqslant G_{\min}, \\ \frac{G-G_{\min}}{G_{\max}-G} & G_{\min} < G < G_{\max}, \\ 1.0 & G \geqslant G_{\max}, \end{cases} \tag{20}$$

and $G_{\min}$ and $G_{\max}$ are calculated, respectively, as (Wong et al., 1990)

$$G_{\min} = \frac{\sqrt{gD\rho_{\text{G}}(\rho_{\text{L}}-\rho_{\text{G}})}}{x}\left(\frac{1}{0.65+1.11X_{\text{tt}}^{0.6}}\right)^2 \tag{21}$$

and

$$G_{\max} = \left\{\frac{gD^{1.2}\rho_{\text{L}}(\rho_{\text{l}}-\rho_{\text{G}})}{0.092(1-X_{\text{tt}})^{1.8}\mu_{\text{L}}^{0.2}}\left[-0.3470+0.2920\ln(X_{\text{tt}})-0.0556\ln^2(X_{\text{tt}})\right]\right\}^{0.556}. \tag{22}$$

Fig. 11 shows the experimental values for CHF compared with the predicted values of the Groeneveld–Cheng–Doan method. Although the predicted errors of certain data are quite large,

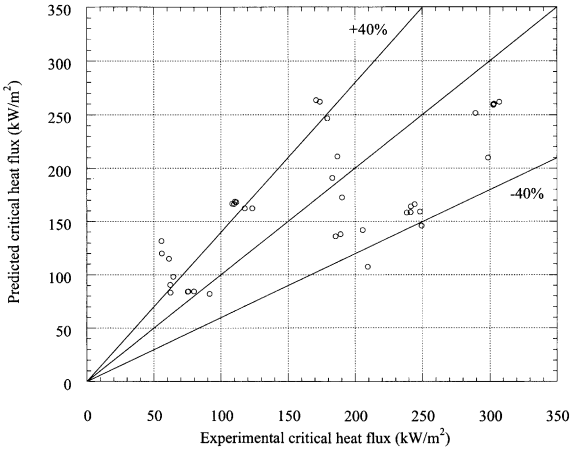

Fig. 11. CHF data compared with predictions of Groeneveld–Cheng–Doan method.

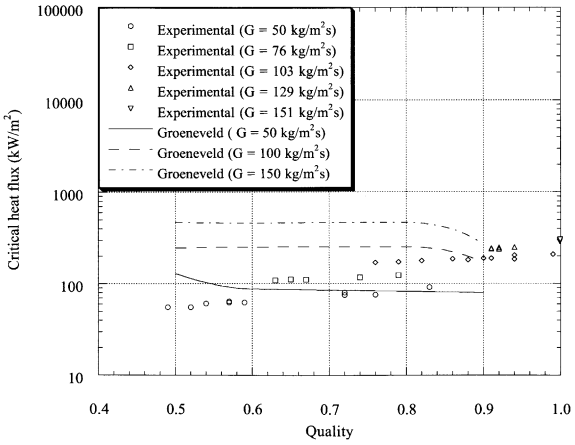

Fig. 12. CHF as a function of mass quality.

the Groeneveld–Cheng–Doan correlation predictions give the right trends for CHF in the present study. The CHF data trends discussed previously are evident in the CHF data of Fig. 12, where it is seen that CHF decreases as mass flux decreases, and this trend is predicted by the Groeneveld–Cheng–Doan correlation. However, this trend is opposite to that found in large tubes at high pressure and high mass fluxes (Tong, 1972). It is also seen in Fig. 12 that the CHF qualities in this study were relatively high (above 0.5) when compared with large-diameter-tube data (Tong, 1972).

5. Conclusions

In general, the data of this study for boiling water in a small 2.98-mm-diameter channel differed from predictions based on larger-channel studies. The pressure gradient and heat transfer coefficient results were successfully correlated with modifications of existing correlations developed for either water boiling in larger channels or refrigerants boiling in small channels. Differences were also found between the present data and larger tube CHF results. In conclusion, the following specific statements can be made.

The two-phase pressure drop data of the small channel of this study were consistently lower than would be expected in larger channels at the same mass fluxes. This comparison came from the widely used Chisholm correlation for larger channels and was attributed to two-phase flow regime differences between the channel sizes. A modification of the Chisholm correlation was developed to better predict activity in small-diameter channels.

Boiling heat transfer of water in the small channel of this study was found to be heat-flux-dependent but essentially mass-flux-independent. This trend is consistent with refrigerant boiling in small channels but significantly different from larger-channel boiling, where the mass flux effect may dominate. This result translates to a dominance of the nucleation heat transfer mechanism over the convective mechanism in small channels, and it persisted to high qualities above 0.5. A new correlation for two-phase heat transfer coefficient for water flow boiling in a small horizontal channel was developed based on boiling results with refrigerants under similar conditions.

It was found that CHF occurred at relatively high qualities between 0.5 and 1.0 for water in the 2.98-mm-inside-diameter horizontal channel of this study. Such qualities are higher than those found in large tubes (at higher pressures and mass fluxes). The CHF quality was found to decrease with decreased mass flux, and this trend is opposite to that found in larger tubes. The Groeneveld–Cheng–Doan method, based on a lookup table value and mass flux correction for horizontal flow, provides an approximation of the CHF of the present study with correct trends for small tubes.

Acknowledgements

This work was supported by the US Department of Energy, Offices of Heavy Vehicle Technologies and Advanced Automotive Technologies, under contract W-31-109-Eng-38. The authors thank Roger K. Smith for his contributions in fabrication of the test apparatus and in the conduct of the experiments, and Joyce Stephens for help in preparing the manuscript and associated graphics.

References

ASHRAE, 1993. Handbook of Fundamentals. ASHRAE, Atlanta, GA.

Chen, J.C., 1966. A correlation for boiling heat transfer to saturated fluids in convective flow. I & EC Process Des. Develop. 5, 322–329.

Chisholm, D., 1967. A theoretical basis for the Lockhart–Martinelli correlation for two-phase flow. Int. J. Heat Mass Transfer 10, 1767–1778.

Chisholm, D., 1973. Pressure gradients due to friction during the flow of evaporating two-phase mixtures in smooth tubes and channels. Int. J. Heat Mass Transfer 16, 347–358.

Dittus, F.W., Boelter, L.M.K., 1930. Heat transfer in automobile radiators of the tubular type. Univ. Californ. Publ. Eng. 2, 443–461.

Forster, H.K., Zuber, N., 1955. Dynamics of vapor bubbles and boiling heat transfer. AIChE J. 1, 531.

Groeneveld, D.C., Cheng, S.C., Doan, T., 1986. 1986 AECL-UO critical heat flux lookup table. Heat Transfer Eng. 7, 46–62.

Lockhart, R.W., Martinelli, R.C., 1949. Proposed correlation of data for isothermal two-phase two-component flow in pipes. Chem. Eng. Prog. 45, 39–48.

Moffat, R.J., 1988. Describing the uncertainties in experimental results. Exp. Thermal Fluid Sci. 1, 3–17.

Petukhov, B.S., 1970. Heat transfer and friction in turbulent pipe flow with variable physical properties. In: Advances in Heat Transfer, vol. 6. Academic Press, New York, pp. 503–564.

Tong, L.S., 1972. Boiling Crisis and Critical Heat Flux. US Atomic Energy Commission.

Tran, T.N., Wambsganss, M.W., France, D.M., 1996. Small circular- and rectangular-channel boiling with two refrigerants. Int. J. Multiphase Flow 22, 485–498.

Wambsganss, M.W., Jendrzejczyk, J.A., France, D.M., 1992. Two-phase flow and pressure drop in flow passages of compact heat exchangers. SAE Technical Paper 920550.

Weisman, J., 1992. The current status of theoretically based approaches to the prediction of the critical heat flux in flow boiling. Nucl. Technol. 9, 1–21.

Wong, Y.L., Groeneveld, D.C., Cheng, S.C., 1990. CHF prediction for horizontal tubes. Int. J. Multiphase Flow 16, 123–138.